

PAPER • OPEN ACCESS

Thermal acclimation of plant photosynthesis and autotrophic respiration in a northern peatland

To cite this article: Shuang Ma *et al* 2023 *Environ. Res.: Climate* **2** 025003

View the [article online](#) for updates and enhancements.

You may also like

- [Acclimation of *Juglans mandshurica* Maxim. and *Phellodendron amurense* Rupr. in the Middle Volga region](#)
D Tishin, M Fardeeva, N Chizhikova et al.
- [The health burden of fall, winter and spring extreme heat events in Southern California and contribution of Santa Ana Winds](#)
Lara Schwarz, Brian Malig, Janin Guzman-Morales et al.
- [Denitrification performance of acclimated bio-floc in sequencing batch reactor](#)
Tao Wang, Qingsong Liu, Hua Li et al.

ENVIRONMENTAL RESEARCH CLIMATE



PAPER

OPEN ACCESS

RECEIVED
30 November 2022

REVISED
21 February 2023

ACCEPTED FOR PUBLICATION
22 March 2023

PUBLISHED
21 April 2023

Original content from
this work may be used
under the terms of the
[Creative Commons
Attribution 4.0 licence](#).

Any further distribution
of this work must
maintain attribution to
the author(s) and the title
of the work, journal
citation and DOI.



Thermal acclimation of plant photosynthesis and autotrophic respiration in a northern peatland

Shuang Ma^{1,2,*}, Lifan Jiang^{3,*}, Rachel M Wilson⁴, Jeff Chanton⁴, Shuli Niu⁵, Colleen M Iversen⁶, Avni Malhotra^{6,7}, Jiang Jiang⁸, Yuanyuan Huang⁹, Xingjie Lu¹⁰, Zheng Shi¹¹, Feng Tao¹², Junyi Liang¹³, Daniel Ricciuto⁶, Paul J Hanson⁶ and Yiqi Luo^{3,*}

¹ Center for Ecosystem Science and Society, Department of Biological Sciences, Northern Arizona University, Flagstaff, AZ, United States of America

² Jet Propulsion Laboratory, California Institute of Technology, Pasadena, CA, United States of America

³ School of Integrative Plant Science, Cornell University, Ithaca, NY, United States of America

⁴ Earth, Ocean and Atmospheric Sciences, Florida State University, Tallahassee, FL, United States of America

⁵ Key Laboratory of Ecosystem Network Observation and Modeling, Institute of Geographic Sciences and Natural Resources Research, Chinese Academy of Sciences, Beijing, People's Republic of China

⁶ Environmental Sciences Division and Climate Change Science Institute, Oak Ridge National Laboratory, Oak Ridge, TN, United States of America

⁷ Department of Geography, University of Zurich, Zurich, Switzerland

⁸ Department of Soil and Water Conservation, Nanjing Forestry University, Nanjing, Jiangsu, People's Republic of China

⁹ CSIRO Oceans and Atmosphere, Aspendale, Victoria, Australia

¹⁰ School of Atmospheric Sciences, Sun Yat-sen University, Guangzhou, Guangdong, People's Republic of China

¹¹ Department of Microbiology and Plant Biology, University of Oklahoma, Norman, OK, United States of America

¹² Ministry of Education Key Laboratory for Earth System Modeling, Department of Earth System Science, Tsinghua University, Beijing, People's Republic of China

¹³ Department of Grassland Resource and Ecology, China Agricultural University, Beijing, People's Republic of China

* Authors to whom any correspondence should be addressed.

E-mail: shuang.ma@jpl.nasa.gov, lj289@cornell.edu and yl2735@cornell.edu

Keywords: autotrophic respiration, data-model fusion, peatland, photosynthesis, thermal acclimation, warming

Abstract

Peatlands contain one-third of global soil carbon (C), but the responses of peatland ecosystems to long-term warming are not well understood. Here, we pursue an emergent understanding of warming effects on ecosystem C fluxes at peatlands by constraining a process-oriented model, the terrestrial ECOsystem model, with observational data from a long-term warming experiment at the Spruce and Peatland Responses Under Changing Environments site. Model-based assessments show that ecosystem-level photosynthesis and autotrophic respiration exhibited significant thermal acclimation, with temperature sensitivities being linearly decreased with warming. Using the thermal-acclimated parameter values, simulated gross primary production, net primary production, and plant autotrophic respiration (R_a), were all lower than those simulated with non-thermal acclimated parameter values. In contrast, ecosystem respiration simulated with thermal acclimated parameter values was higher than that simulated with non-thermal acclimated parameter values. Net ecosystem CO_2 exchange was much higher after constraining model parameters with observational data from the warming treatments, releasing C at a rate of $28.3 \text{ g C m}^{-2} \text{ yr}^{-1} \text{ }^\circ\text{C}^{-1}$. Our data-model integration study suggests that peatlands are likely to release more C than previously estimated. Earth system models may overestimate C uptake by peatlands under warming if physiological thermal acclimation of plants is not incorporated. Thus, it is critical to consider the long-term physiological thermal acclimation of plants in the models to better predict global C dynamics under future climate and their feedback to climate change.

1. Introduction

Peatlands play an important role in the global carbon cycle. Peatlands are a major global carbon (C) sink, containing one-third of global soil C due to the slow decomposition of organic matter under cold, water-saturated, and oxygen-limited conditions (Bridgman *et al* 2006). On the other hand, peatlands emit a substantial amount of methane (CH₄) into the atmosphere each year (Abdalla *et al* 2016, Ma *et al* 2021). The exclusion of peatland C dynamics, including shifts in greenhouse gas emissions, from the majority of Earth system models (ESMs) involved in the Coupled Model Intercomparison Project Phase 6 may contribute to the large uncertainty in ESM projections and low confidence in the magnitude of global soil C losses under warming (IPCC 2021). Therefore, it is critical to understand how peatland ecosystem processes respond to long-term (years to decades) warming so that we can better predict future global carbon fluxes between the atmosphere and Earth's surface and their feedbacks (Smith and Dukes 2013).

Some individual ecological processes of peatlands under long-term warming, e.g. fine-root growth (Malhotra *et al* 2020), nutrient cycling (Iversen *et al* 2022), and incorporation and degradation of plant- and microbe-derived organic matter (Ofiti *et al* 2022), have recently been studied owing to a long-term, whole-ecosystem climate change experiment, i.e. the Spruce and Peatland Responses Under Changing Environments (SPRUCEs) experiment in a peatland ecosystem in Minnesota, USA. Carbon stocks and fluxes at the ecosystem level, including methane emissions, in response to long-term warming have also been investigated under this project (Griffiths *et al* 2017, Ma *et al* 2017, Jiang *et al* 2018, Hanson *et al* 2020, Ricciuto *et al* 2021, Yuan *et al* 2021). Net ecosystem production shifted significantly toward a smaller C sink or a minor C source under the most extreme experimental warming scenario (i.e. +9 °C warming scenario; Hanson *et al* 2020). However, peatland ecosystem-level plant physiological responses to long-term warming remain unclear.

Physiological mechanisms for instantaneous temperature responses of C exchange processes of plants are relatively well-studied at the leaf level. For example, it has been widely reported that increased temperature stimulates enzyme activities up to an optimum temperature, which then declines due to enzymatic degradation at higher temperatures (Niu *et al* 2012, Smith and Dukes 2013). Compared to the leaf level, less is known about ecosystem-level C exchange responses to warming, especially in the long term (Bradford *et al* 2008, Ziehn *et al* 2011, Lombardozzi *et al* 2015, Smith *et al* 2015). Empirical evidence indicates that the initial increase in ecosystem fluxes such as soil or ecosystem respiration (ER) under warming can decline or disappear after a certain time (Luo *et al* 2001, Melillo *et al* 2002, Eliasson *et al* 2005). Such changes in C cycling responses to warming can be attributed to physiological acclimation, species composition change, or altered substrate availability (Bradford *et al* 2008, Smith and Dukes 2013).

The down-regulation of temperature-adapted physiological behavior, which is defined as thermal acclimation, may lead to the observed C flux responses to temperature (apparent acclimation) or slow down the increasing trend of C fluxes (non-apparent acclimation) in a warmer climate (Oechel *et al* 2000, Davidson and Janssens 2006). Thermal acclimation of plant photosynthesis and autotrophic respiration has frequently been reported (e.g. Campbell *et al* 2007, Smith and Dukes 2013, Smith *et al* 2015, 2019, Kumarathunge *et al* 2019). As a result of such acclimation, simulated C sensitivity to climate was significantly reduced (Smith *et al* 2015, Liang *et al* 2018). Therefore, failure to account for acclimation of plant photosynthesis and autotrophic respiration may cause bias in simulating land C cycling (Smith and Dukes 2013, Smith *et al* 2015, Liang *et al* 2018, 2019). More and more models have incorporated dynamic parameterization that allows models to simulate the thermal acclimation of plant photosynthesis and autotrophic respiration (Atkin *et al* 2014, Lombardozzi *et al* 2015, Huntingford *et al* 2017).

Photosynthetic thermal acclimation is primarily controlled by photosynthetic biochemistry, although stomatal regulation and daytime respiration also contribute (Lin *et al* 2013, Kumarathunge *et al* 2019). The algorithms used for approximating photosynthetic acclimation to temperature emerged only recently, primarily due to the lack of empirical data for temperature-responsive variables such as the maximum carboxylation rate at reference temperature (V_{cmaxref}), usually 25 °C and the maximum potential rate of electron transport at a reference temperature (J_{maxref}), which are most commonly used in implementations of the Farquhar photosynthesis model (Farquhar *et al* 1980) in most ESMs (Kattge and Knorr 2007, Friend 2010, Scafaro *et al* 2017). V_{cmaxref} and J_{maxref} represent basal values of photosynthetic capacity while activation energy (E_a), deactivation energy (E_b), and entropy (ΔS) describe the direct effect of temperature on photosynthetic capacity (Stinziano *et al* 2018). Hikosaka (2006) identified two responsive variables for photosynthetic thermal acclimation of 23 C₃ species based on empirical data: activation energy of V_{cmaxref} (E_{aV}) and J_{maxref} (E_{aJ}), as well as the ratio of J_{maxref} to V_{cmaxref} (J/V). Later, linear regressions of J/V and entropy of V_{cmax} (ΔS_V) and J_{max} (ΔS_J) against plant growth temperature (T_{growth}) were derived for 36 species, whereas no significant correlation between E_a and T_{growth} among these species was found (Kattge and Knorr 2007). The generalized linear regression models have widely been used in large-scale and global

modeling studies (Ziehn *et al* 2011, Arneth *et al* 2012, Lombardozzi *et al* 2015, Smith *et al* 2015). The most comprehensive analysis of the photosynthetic temperature responses covered 141 species from tundra to tropical forest (Kumarathunge *et al* 2019), in which ΔS_V , ΔS_J , $J_{\max\text{ref}}$, and J/V all declined but V_{cmaxref} did not change with increasing T_{growth} . Kumarathunge *et al* (2019) also found an increase in E_{aV} but no change in E_{aJ} with increasing T_{growth} . The aforementioned studies described thermal acclimation as a function of T_{growth} and responsive variables, such as J/V and temperature sensitivity (Q_{10}). More empirical data are needed to generalize the key model parameters (e.g. V_{cmaxref}) to accurately simulate long-term feedbacks between the atmosphere and terrestrial ecosystems (TECOs) under climate warming.

Dynamic parameterization has also been incorporated to allow models to simulate the thermal acclimation of plant autotrophic respiration (Atkin *et al* 2014, Lombardozzi *et al* 2015, Huntingford *et al* 2017). Early studies aimed to represent the dynamic responses of autotrophic respiration to temperature using a temperature-dependent Q_{10} , instead of a fixed value, to capture the instantaneous responses of autotrophic respiration observed in the field (Larcher 1980). Other studies used algorithms to characterize respiratory acclimation to longer-term growth conditions (King *et al* 2006, Atkin *et al* 2008). The algorithms used by King *et al* (2006) and Atkin *et al* (2008) were both derived from empirical data in warming experiments with multiple species that covered different functional groups. However, more empirical research is needed to quantify the dynamic responses of plant respiration to temperature across a wider range of species, plant functional types, and environmental conditions.

The lack of empirical data for identifying the key variables of thermal acclimation has become a barrier to the realistic representations of thermal acclimation of plant photosynthesis and autotrophic respiration in models. While more observations and experiments are needed for deriving the temperature-responsive variables, an alternative approach, data-model fusion, can help obtain those temperature-responsive variables. Data-model fusion assimilates empirical data from multiple sources into process-based biogeochemical models to constrain model parameters (Luo and Schuur 2020), including parameters describing thermal acclimation of plant physiological processes (e.g. basal photosynthetic rate and Q_{10}). For example, a data-model fusion study in Arctic tundra showed that warming increased the light-use efficiency of vegetation but decreased the baseline turnover rate of both labile and recalcitrant soil organic carbon (SOC) pools, suggesting that physiological acclimation in plants and functional gene shifts in microbes occurred (Liang *et al* 2018).

To examine how ecosystem fluxes of peatlands responded to long-term warming, in this study, we assimilated observational data from the SPRUCE experiment to a process-based biogeochemistry model, the TECO model, specialized for the SPRUCE site (TECO_SPRUCE). We hypothesized that plant physiological processes such as photosynthesis and autotrophic respiration exhibit thermal acclimation under long-term warming.

2. Materials and methods

2.1. Site description and measurements

The empirical data used in this modeling study were measured from the SPRUCE experiment (Hanson *et al* 2017; <http://mnspruce.ornl.gov>). The experiment site is a precipitation-fed, ombrotrophic bog in northern Minnesota, USA (N 47° 30.476', W 93° 27.162'). The mean annual temperature was 3.4 °C and the mean annual precipitation was 780 mm from 1961 to 2009 (Sebestyen *et al* 2011). The mean peat depth is 2–3 m due to historical accumulation of peat under cold, anaerobic conditions (Parsekian *et al* 2012). The site includes the dominant tree species, *Picea mariana* and *Larix laricina*, a variety of ericaceous shrubs, such as *Rhododendron groenlandicum* and *Chamaedaphne calyculata*, herbaceous perennials *Eriophorum vaginatum*, *Carex trisperma*, and *Maianthemum trifolium*, as well as a dense layer of *Sphagnum* sp. moss. The herbaceous plants have seasonal dieback of their aboveground tissues.

An ecosystem-level manipulation was implemented at this site to study the responses of the northern peatland ecosystems to climate warming and elevated atmospheric CO₂ (Hanson *et al* 2017). For this specific study, we focused on warming treatments only.

A gradient of warming treatments, including controls, ambient (+0), +2.25, +4.5, +6.75, and +9 °C warming is implemented in open-top chambers (12 m in diameter and ~8 m in height). The control refers to the plot with no open-top chamber whereas the ambient refers to the plot covered by an open-top chamber but with no warming. Each of the warming enclosures is heated both above- and below-ground at the same target temperatures. Deep peat warming began in June of 2014, and target temperatures were achieved at a depth of 2 m. The aboveground warming started in August of 2015, and the target temperatures were controlled at 2 m above ground. Air temperature in the control plots without chambers is approximately 2 °C lower than the ambient plots with chambers but no heating due to the heating effect of the chamber. Thus, the ambient plots are considered the lowest warming treatment in this study and are named +0 °C.

Table 1. The observational data measured in the SPRUCE experiment and used in this study.

Purpose	Data	Year	Period	Time step	References
Environmental variables (model input) to drive the TECO-SPRUCE model, spin up and forward run	Soil temperature at 0, 5, 10, 20, 30, 40, 50, 100, 200 cm depths Air temperature at 2 m Relative humidity at 2 m height Wind speed at 10 m height Precipitation Photosynthetically active radiation (PAR) at 2 m height	2011–2018	Whole year	Hourly	Hanson <i>et al</i> (2015a, 2015b) Hanson <i>et al</i> (2016b)
Water balance calibration	Soil moisture at 0 and 20 cm depth Water table depth	2014–2018	Whole year	Hourly	Hanson <i>et al</i> (2015a, 2015b) Hanson <i>et al</i> (2016b)
Data streams used in data-model fusion	Leaf, wood, root biomass Soil carbon content NEE, GPP, ER	2014–2018 2012 2015–2018	End of growing season August 13–15 Growing season	Once a year One time 1–2 times a month	Hanson <i>et al</i> (2018a, 2018b) Norby <i>et al</i> (2018) Iversen <i>et al</i> (2014) Hanson <i>et al</i> (2014) Hanson <i>et al</i> (2016a)

The environmental variables measured in 2011–2014 from the earliest control plot were used to spin up the TECO_SPRUCE model to a steady state. The environmental variables from each warming plot from 2015 to 2018 were used as model input (table 1). Instead of simulating temperature in different peat layers, we used the measured temperatures half-hourly at 0, –5, –10, –20, –30, –40, –50, –100, and –200 cm depths and aggregated them into hourly intervals to drive the model because the peat was heated to the target temperatures at a 2 m depth. Soil moisture of different soil layers and water table depths from individual plots in 2014–2018 were used to calibrate the modeled water-heat balance. We used ecosystem-level C pools (leaf, wood, root, and SOC) and fluxes, including gross primary production (GPP), net ecosystem CO₂ exchange (NEE), and ER, of the shrub ecosystems from 2015 to 2018 for data-model fusion (Hanson *et al* 2016a, Norby *et al* 2019). These fluxes were measured at least once a month during snow-free months from 2015 to 2018 with a portable open-path analyzer attached to a chamber (1.2 m in diameter). The chamber was put on the soil surface within the plots and covered the shrubs. Data points measured within an hour were averaged as hourly measurements for each plot to match model's time step for data-model fusion as well as model evaluation. Finally, about 30 data points from each plot were used to compare with hourly model output for data-model fusion. A complete list of the data streams used as observations to constrain model parameters is in table 1.

2.2. Model description

We used a process-based biogeochemistry model, TECO_SPRUCE, for our data-model fusion study. The model was built with six major modules working at an hourly time step: canopy photosynthesis, soil water dynamics, plant growth, soil thermal dynamics, soil carbon/nitrogen (N) transfer, and soil CH₄ dynamics. A detailed description of these modules can be found in Weng and Luo (2008), Shi *et al* (2015), Jiang *et al* (2018), Huang *et al* (2017) and Ma *et al* (2017, 2022). Here, we briefly describe these modules and highlight the instantaneous temperature response functions for photosynthesis and autotrophic respiration.

The canopy photosynthesis module was mainly derived from a two-leaf model which coupled surface energy, water, and carbon fluxes (Wang and Leuning 1998). Leaf photosynthesis was calculated based on the Farquhar photosynthesis model (Farquhar *et al* 1980) and the stomatal conductance model (Ball *et al* 1987). The temperature responses of parameters V_{cmax} (maximum rate of carboxylation) and J_{max} (maximum potential rate of electron transport) varied with leaf temperature following the modified Arrhenius function (Johnson *et al* 1942):

$$V_{\text{cmax}} = V_{\text{cmaxref}} * f(T_{\text{leaf}}), \quad (1)$$

$$J_{\text{max}} = V_{\text{cmaxref}} * \frac{J}{V} * f(T_{\text{leaf}}), \quad (2)$$

$$f(T_{\text{leaf}}) = \exp\left[\frac{\Delta H_a (T_{\text{leaf}} - T_{\text{ref}})}{T_{\text{ref}} R_{\text{gas}} T_{\text{leaf}}}\right] \frac{1 + \exp\left(\frac{T_{\text{ref}} \Delta S - \Delta H_d}{T_{\text{ref}} R_{\text{gas}}}\right)}{1 + \exp\left(\frac{T_{\text{leaf}} \Delta S - \Delta H_d}{T_{\text{leaf}} R_{\text{gas}}}\right)}, \quad (3)$$

where V_{cmaxref} is V_{cmax} at reference temperature (293.2 K), T_{leaf} is leaf temperature (K), $f(T_{\text{leaf}})$ is the factor of leaf temperature (unitless), J/V is the ratio of J_{maxref} to V_{cmaxref} , ΔH_a is the activation energy (J mol^{-1}), T_{ref} is reference temperature of leaf (K), R_{gas} is the gas constant ($8.314 \text{ J K}^{-1} \text{ mol}^{-1}$), ΔS is entropy ($\text{J K}^{-1} \text{ mol}^{-1}$), and ΔH_d is the deactivation energy (J mol^{-1}). ΔS used in equations (1) and (2) have slightly different values, where Entropy of J_{max} (ΔS_j) is derived from Entropy of V_{cmax} (ΔS_v): $\Delta S_j = \Delta S_v * 668/664$. According to Kattge and Knorr (2007), the photosynthetic acclimation to growth temperature is reflected by changing values of ΔS and J/V . Thus, in this study, instead of using a constant value for ΔS and J/V , we set these parameters to be variable within a prior range, which could be constrained by the observation data.

The water table level was estimated using a simple bucket model as described by Granberg *et al* (1999). The plant growth module calculated the allocation of photosynthesis C to plant pools (leaf, stem, and root), plant growth, plant autotrophic respiration, phenology, and C transfer to litter and soil pools. The autotrophic respiration of leaf, stem, and root was calculated as:

$$Rm_{\text{leaf}} = R_{0\text{leaf}} * S_{\text{NR}_a} * \text{leafC} * Q_{10\text{Ra}}^{\frac{T_{\text{air}}-10}{10}} * \text{fnsc}, \quad (4)$$

$$Rm_{\text{stem}} = R_{0\text{stem}} * S_{\text{NR}_a} * \text{stemsapC} * Q_{10\text{Ra}}^{\frac{T_{\text{air}}-25}{10}} * \text{fnsc}, \quad (5)$$

$$Rm_{\text{root}} = R_{0\text{root}} * S_{\text{NR}_a} * \text{rootsapC} * Q_{10\text{Ra}}^{\frac{T_{\text{air}}-25}{10}} * \text{fnsc}, \quad (6)$$

where Rm_{leaf} , Rm_{stem} , and Rm_{root} are maintenance respiration rates of leaf, stem and root, respectively ($\text{g C m}^{-2} \text{ h}^{-1}$), $R_{0\text{leaf}}$, $R_{0\text{stem}}$, and $R_{0\text{root}}$ are basal respiration rates of leaf, stem and root, respectively ($\text{g respired C g}^{-1} \text{ biomass C m}^{-2} \text{ h}^{-1}$), S_{NR_a} is the nitrogen scaler for autotrophic respiration (unitless), leafC , stemsapC , rootsapC are C content of leaf, stem sapwood, and root sapwood, respectively (g C m^{-2}), $Q_{10\text{Ra}}$ is temperature sensitivity of autotrophic respiration (unitless), T_{air} is air temperature, and fnsc is the scaling factor of nonstructural C pool (unitless). We set prior ranges for basal respiration rates of leaf, stem, and root and temperature sensitivity of autotrophic respiration and they could be constrained by the observation data.

2.3. Data-model fusion

We applied the Metropolis-Hasting algorithm (Metropolis *et al* 1953) to generate the posterior distribution of parameters. We assumed a uniform distribution for the prior range of each parameter so that the chance of each value being accepted is equal. We also assumed that errors between observations and model simulations independently follow a normal distribution with a zero mean. The cost function weights the mismatch between the multiple observational data streams and the modeled corresponding variables, represented by:

$$p(\theta) \propto \exp \left\{ - \sum_{i=1}^7 \sum_{t \in Z_i} \frac{[Z_i(t) - X(t)]^2}{2\sigma_i^2(t)} \right\}, \quad (7)$$

where $Z_i(t)$ is the i th observation stream at time t , $X(t)$ is the corresponding simulated value, and $\sigma_i(t)$ is the standard deviation of observational error estimates. There were seven observational data streams used in total (table 1).

We generated the posterior distributions of parameter values using 50 000 iterations during the optimization process. The parameter value at the current step was based on the accepted parameter value in the previous step. The current value was accepted only if the mismatch between the observation and model simulation was reduced or otherwise randomly accepted with a 0.05 probability. We used the Gelman-Rubin statistic (Gelman and Rubin 1992) to examine the convergence of sampling chains. The first half of the accepted parameter values were discarded from the burn-in period, and the second half of the accepted parameter values were used for posterior analysis. More details on sampling and the cost function can be found in Xu *et al* (2006).

Under photosynthetic thermal acclimation, the ratio of J_{maxref} and V_{cmaxref} (i.e. J/V), ΔS_v , and ΔS_j have consistently been found to change with growth temperature across different studies, but activation energy (ΔH_a) did not change with growth temperature (Hikosaka *et al* 2006, Kattge and Knorr 2007, Kumarathunge *et al* 2019). Given the limited amount of observational data to constrain the model parameters, if we allowed all the six parameters (J_{maxref} , V_{cmaxref} , ΔS_v , ΔS_j , ΔH_{a_v} , and ΔH_{a_j}) in equation (7) to vary during optimization, the parameter posterior distributions tend to be highly correlated to each other, resulting in poor results. We thus set ΔH_{a_v} and ΔH_{a_j} to be constant and let J_{maxref} , V_{cmaxref} , ΔS_v , and ΔS_j vary. In addition to these four parameters, we selected all other instantaneous temperature-responsive parameters (table 2) that might change due to thermal acclimation according to previous studies to be

Table 2. Parameters included in data-model fusion.

Processes	Parameter	Definition	Unit	Prior range	Reference
Photosynthesis	J/V	The ratio of $J_{\max\text{ref}}/V_{\text{cmaxref}}$	—	[1,3]	Kattge and Knorr (2007)
	V_{cmaxref}	The maximum rate of carboxylation	$\mu\text{mol m}^{-2} \text{s}^{-1}$	[5,80]	Kattge and Knorr (2007)
	ΔS_V	Entropy of V_{cmax}	$\text{J K}^{-1} \text{mol}^{-1}$	[640,670]	Kattge and Knorr (2007)
	ΔS_J	Entropy of J_{\max}	$\text{J K}^{-1} \text{mol}^{-1}$	[648,674]	Kattge and Knorr (2007)
Autotrophic respiration	Q_{10Ra}	Temperature sensitivity of autotrophic respiration	—	[1,4]	Atkin et al (2008)
	R_{l0}	Basal rate of leaf respiration	$\text{g respired C g}^{-1} \text{biomass C m}^{-2} \text{h}^{-1}$	[10,45]	Atkin et al (2008), Jiang et al (2018)
	R_{s0}	Basal rate of stem respiration	$\text{g respired C g}^{-1} \text{biomass C m}^{-2} \text{h}^{-1}$	[5,10]	Atkin et al (2008), Jiang et al (2018)
	R_{r0}	Basal rate of root respiration	$\text{g respired C g}^{-1} \text{biomass C m}^{-2} \text{h}^{-1}$	[10,45]	Atkin et al (2008), Jiang et al (2018)
Phenology Pool size-related parameters	g_{ddonset}	Leaf out day of the year	day	[100,160]	Jiang et al (2018)
	GL_{max}	Leaf maximum growth rate	$\text{g new C g}^{-1} \text{biomass C yr}^{-1}$	[10,50]	Jiang et al (2018)
	GS_{max}	Stem maximum growth rate	$\text{g new C g}^{-1} \text{biomass C yr}^{-1}$	[10,30]	Jiang et al (2018)
	GR_{max}	Root maximum growth rate	$\text{g new C g}^{-1} \text{biomass C yr}^{-1}$	[10,30]	Jiang et al (2018)
	τ_{leaf}	Leaf C turnover time	yr	[0.3,3]	Jiang et al (2018)
	τ_{stem}	Stem C turnover time	yr	[1,100]	Jiang et al (2018)
	τ_{root}	Root C turnover time	yr	[0.3,2]	Jiang et al (2018)

constrained by observation data. Additionally, parameters related to changes in C pool size, such as turnover time, allocation factor from/to labile soil C pool, and maximum growth rate of leaf, stem, and root C, were also selected for data-model fusion. We selected 15 parameters in total and detailed information on these parameters and their prior ranges are listed in table 2. The prior ranges of parameters were based on empirical measurements or modeling studies from peatland ecosystems. Indeed, in our test runs of the data-model fusion, we also included all the allocation parameters of plant C pools to vary but having too many parameters to vary at the same time might obscure the limited information contained in observation data streams, especially with limited data points. We thus set constant allocation parameters of plant C pools.

We randomly saved 500 sets of the simulation results from each data-model fusion and calculated the mean value and standard deviation of each parameter to analyze the responses of ecosystem C fluxes to long-term warming and the potential shifts in the parameter values due to thermal acclimation. We further explored how changes in parameters due to physiological thermal acclimation could influence the ecosystem C fluxes of peatlands. Here we used ‘thermal acclimated parameters’ and ‘non-thermal acclimated parameters’ to refer to parameter values constrained by assimilating observation data from warming (indicated by color lines in figure 1) and control plots, respectively. Specifically, we ran the model with both non-thermal acclimated and thermal acclimated parameter values and compared the results of the two runs. Both runs used the initial conditions in the control plot, driven by six sets of drivers corresponding to six warming treatments.

2.4. Statistical analyses

To evaluate model performance in simulating C fluxes, linear regressions were performed to compare simulated and observed C fluxes. The observed C fluxes used for evaluation are the same C fluxes as used for constraining the TECO model, which were measured 1–2 times a month during growing seasons from 2015 to 2018 in each plot. Root mean square error (RMSE) was calculated to evaluate model performance against the observation data.

To test the possible thermal acclimation of plant physiology, we performed linear regressions between model parameters and temperature, using yearly average of parameters and temperature, including all

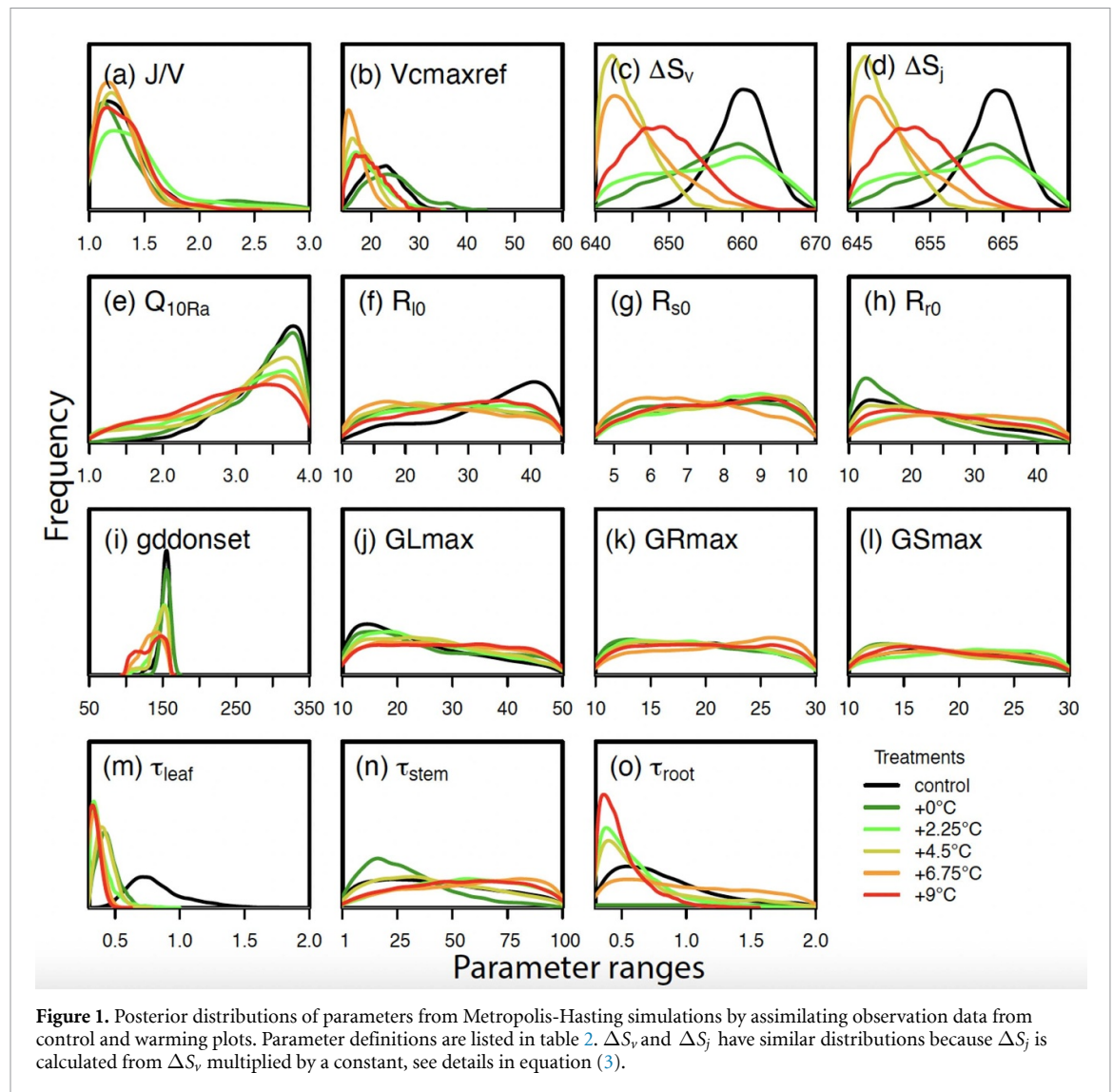


Figure 1. Posterior distributions of parameters from Metropolis-Hasting simulations by assimilating observation data from control and warming plots. Parameter definitions are listed in table 2. ΔS_v and ΔS_j have similar distributions because ΔS_j is calculated from ΔS_v , multiplied by a constant, see details in equation (3).

control and warming treatments from 2016 to 2018. Lastly, we analyzed the dependency of the simulated annual C fluxes on the mean annual temperature including all treatments from 2016 to 2018, in which actual mean annual air temperatures were used as independent variables. All statistical analyses were performed with R software (version 3.6.1, R Core Team 2017).

3. Results

3.1. Parameters constrained by data-model fusion

Among the 15 parameters, eight parameters, J/V , $V_{cmaxref}$, ΔS_v , ΔS_j , Q_{10Ra} , $gddonset$, τ_{leaf} , and τ_{root} , were well constrained by the observational data streams across all treatments, with a unimodal-shaped posterior distribution (table 2, figure 1). The model using optimized parameters by data assimilation fitted the observational data well with RMSE between 0.047 and 0.126 (figure 2).

The correlations between parameter mean values of the posterior distributions and mean annual temperature including all treatments from 2016 to 2018, during which the whole-ecosystem warming treatments were active all year round, were shown in figure 3. The instantaneous temperature responsive parameters of photosynthesis, including $V_{cmaxref}$, J_{maxref} (which was calculated by multiplying J/V by $V_{cmaxref}$), entropy of $V_{cmaxref}$ (ΔS_v), and entropy of J_{maxref} (ΔS_j) all linearly decreased with the increasing treatment temperature. Despite being well constrained, J/V did not show a significant correlation with the increasing mean annual air temperature.

While the basal autotrophic respiration rates of leaf, stem, and root were not well constrained (table 2), the temperature sensitivity of autotrophic respiration, Q_{10Ra} , was well constrained and the mean values of the posterior distribution across all treatments exhibited a significant linear decrease with increasing mean annual air temperatures at a rate of $-0.047\text{ }^{\circ}\text{C}^{-1}$ ($P < 0.001$, figure 3).

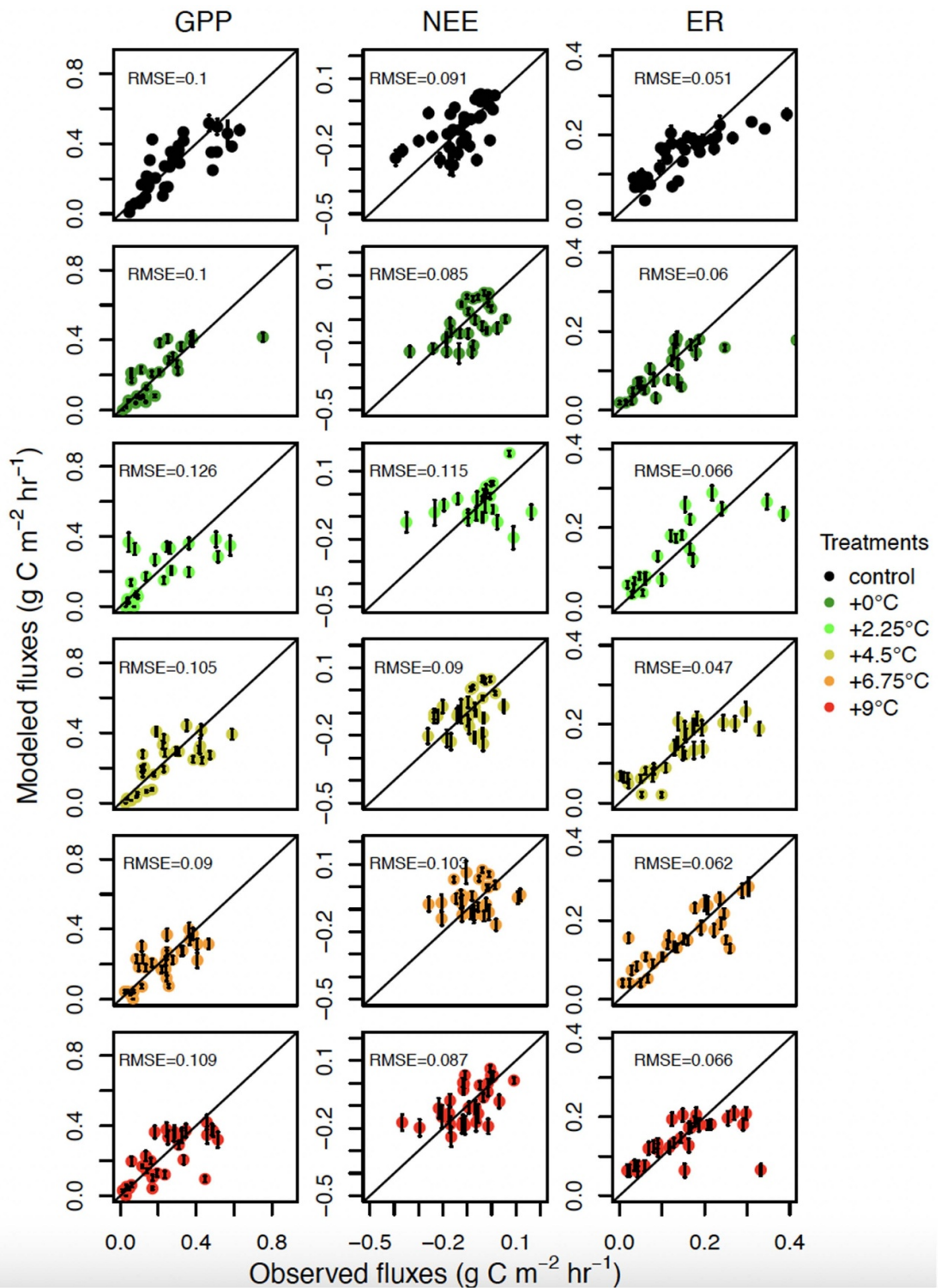


Figure 2. Comparison of observed and model-simulated (mean \pm standard deviation) gross primary production (GPP), net ecosystem CO₂ exchange (NEE), and ecosystem respiration (ER) in the control and warming treatments.

3.2. Simulated ecosystem carbon fluxes under warming

The comparison of C fluxes from 2016 to 2018 simulated with non-thermal acclimated parameter values vs. thermal acclimated parameter values were shown in figure 4. Simulated GPP (figure 4(a)) and net primary production (NPP) (figure 4(b)) using non-thermal acclimated parameter values were higher than those using thermal acclimated parameter values. Moreover, GPP simulated with thermal acclimated parameter values did not change significantly with increasing annual air temperature. In contrast, NPP simulated with thermal acclimated parameter values increased linearly with increasing annual air temperature at a rate of

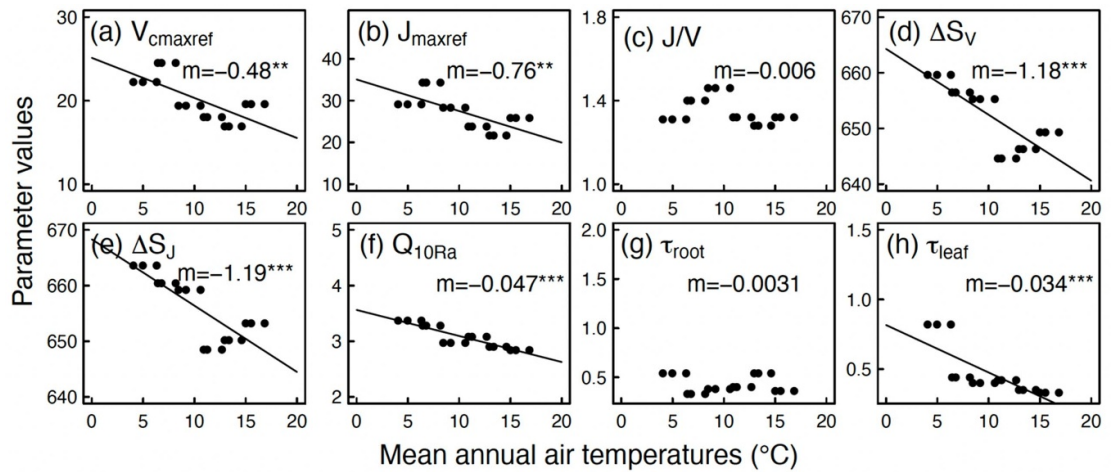


Figure 3. Parameter mean values from well-constrained posterior distributions to characterize the temperature dependence on mean annual air temperature including all control and warming treatments from 2016 to 2018: (a)–(e) are temperature response variables in photosynthesis, (f) is temperature response variable in autotrophic respiration, and (g)–(h) are the turnover time of root and leaf pools in unit of year. Linear regressions are shown in solid lines. The slope (m) of linear regression indicates the magnitude of the parameter in response to increasing mean annual air temperature at 2 m height. *, **, and *** indicate significant levels at 0.05, 0.01, and 0.001, respectively.

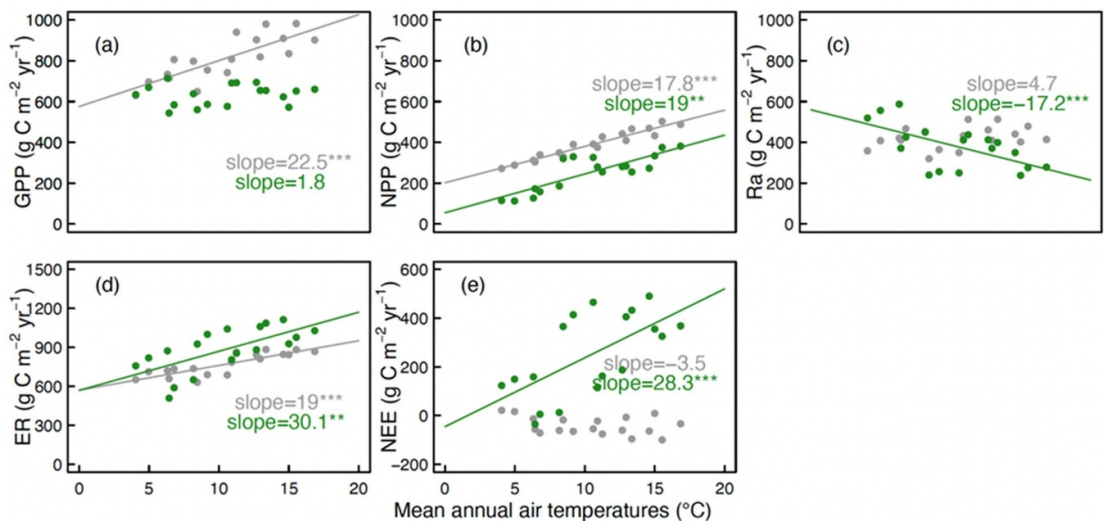


Figure 4. Simulated annual carbon fluxes in relation to mean annual air temperature including all control and warming treatments from 2016 to 2018. Points are mean values from 500 model simulations with parameters randomly drawn from the posterior distributions. Green and gray points are simulated C fluxes with thermal acclimated and non-thermal acclimated parameter values, respectively. Mean annual air temperatures at 2 m height were used for regressions.

$19.0 \text{ g C m}^{-2} \text{ yr}^{-1} \text{ } ^\circ\text{C}^{-1}$ ($P < 0.001$). Similar to GPP and NPP, simulated plant autotrophic respiration, R_a , using non-thermal acclimated parameter values was higher than that using thermal acclimated parameter values (figure 4(c)). R_a simulated using thermal acclimated parameter values decreased linearly as annual air temperature increased by $17.2 \text{ g C m}^{-2} \text{ yr}^{-1} \text{ } ^\circ\text{C}^{-1}$ ($P < 0.001$).

Simulated ER with both non-thermal acclimated and thermal acclimated parameter values increased significantly with annual air temperature, and ER simulated with thermal acclimated parameter values was higher than ER simulated with non-thermal acclimated parameter values (figure 4(d)). Without thermal acclimation (simulations with non-thermal acclimated parameter values), due to significant increases in both GPP and ER at a similar rate, the ecosystem remained a minor C sink, i.e. a negative value of NEE (figure 4(e)). However, after constraining parameters with observational data from the warming treatments, the ecosystem turned from a neutral/minor C sink into a major C source, releasing C at a rate of $28.3 \text{ g C m}^{-2} \text{ yr}^{-1} \text{ } ^\circ\text{C}^{-1}$ ($P < 0.001$; figure 4(e)).

4. Discussion

Peatlands are an important ecosystem in the global C cycle as they store large amounts of soil C, which could be vulnerable to climate change. However, the responses of peatland C cycle to climate change, especially long-term responsive patterns, are poorly understood. In this study, leveraging measured data from a unique manipulative peatland experiment with multiple warming treatments to constrain a process-based ecosystem model, we explored ecosystem C flux response to long-term warming. We found that including representing thermal acclimation in model processes significantly altered ecosystem C flux components in response to warming; ultimately leading to the ecosystem becoming a much higher net C source than if thermal acclimation was excluded from the model. Below we discuss our findings and their implications for land C modeling.

4.1. Thermal acclimation of plant photosynthesis and autotrophic respiration at ecosystem level

Significant linear responses of plant photosynthesis and autotrophic respiration variables, such as J/V and entropy, to increasing growth temperature have been found at the species level (Kattge and Knorr 2007). These linear temperature responses of photosynthesis are affected by a variety of factors (e.g. soil moisture, slow vs. fast-growing strategies, and plant functional types), which are not always been taken into account when reviewing photosynthetic acclimation to temperature across studies (Lin et al 2013). Similarly, the ability of plants to adjust their respiratory rates in response to long-term thermal changes also varied by location (Larigauderie and Körner 1995) and plant functional types (Tjoelker et al 1999, Atkin et al 2006). The linear responsive pattern drawn from the existing studies supports the theory that plants maximize their resources for growth and reproduction through acclimation, and climate alone can be used to predict the optimal rate of photosynthesis and autotrophic respiration of plants (Smith et al 2019). However, such linearity has never been directly tested at the ecosystem level at one site with a gradient of warming treatments. The unique design of the SPRUCE experiment and the use of the data-model fusion approach makes it possible to test whether model parameters related to C fluxes responded linearly or nonlinearly to increasing temperature at the ecosystem scale. We found that after four years of warming treatments, photosynthetic parameters sensitive to temperature, including V_{cmaxref} , J_{maxref} , and entropy, exhibited thermal acclimation, decreasing linearly with increased temperatures (figure 3). In the meta-analysis by Kattge and Knorr (2007) based on 36 different C_3 species from various ecosystem types, they found that the entropy of both V_{cmaxref} (ΔS_V) and J_{maxref} (ΔS_J) declined as growth temperature increased, at a rate of 1.07 and 0.77 $\text{J K}^{-1} \text{mol}^{-1} \text{ }^\circ\text{C}^{-1}$, respectively. A more comprehensive study based on a wide distribution of 141 species, from tundra to tropical forest, concluded that both ΔS_V and ΔS_J decreased linearly with an increase in temperature by 1.5 $\text{J K}^{-1} \text{mol}^{-1} \text{ }^\circ\text{C}^{-1}$ (Kumarathunge et al 2019). Our results based on the regressions between mean values of the posterior distributions against mean annual temperature also showed a significant linear reduction in ΔS_V with a slope of $-1.18 \text{ J K}^{-1} \text{mol}^{-1} \text{ }^\circ\text{C}^{-1}$ and in ΔS_J with a slope of $-1.19 \text{ J K}^{-1} \text{mol}^{-1} \text{ }^\circ\text{C}^{-1}$, both of which lie in the middle of the empirical-based values.

Unlike previous studies, we did not find a significant change in the ratio of J_{maxref} and V_{cmaxref} in response to the change in temperature. Instead, we did find a linear decrease with increased mean annual temperature in both J_{maxref} ($-0.76 \mu\text{mol m}^{-2} \text{ s}^{-1} \text{ }^\circ\text{C}^{-1}$) and V_{cmaxref} ($-0.48 \mu\text{mol m}^{-2} \text{ s}^{-1} \text{ }^\circ\text{C}^{-1}$). The different results for the simulated responses of photosynthesis to temperature change in our study compared with previous studies could be attributed to the adoption of a decreased J/V at the higher temperature, because this ratio is a mathematical term, but it is J_{maxref} and V_{cmaxref} that directly determine the photosynthetic rate. Reducing J_{maxref} alone is likely to reduce total photosynthesis (Arneth et al 2012, Lombardozi et al 2015, Smith et al 2015), whereas increasing V_{cmaxref} alone is likely to increase total photosynthesis (Lin et al 2012). According to Mercado et al (2018), a simultaneous decrease in both J_{maxref} and V_{cmaxref} may be the best way to achieve a decreased J/V . Although we did not find a significant decrease in J/V , our results showed that both J_{maxref} and V_{cmaxref} declined linearly as mean annual temperature increased, which has been proposed by Mercado et al (2018) to account for photosynthetic thermal acclimation.

In our study, the temperature sensitivity of plant autotrophic respiration, Q_{10Ra} , was well-constrained across all the treatments and the mean values of the posterior distribution of Q_{10Ra} declined linearly with an increase of mean annual air temperature at a rate of $0.047 \text{ }^\circ\text{C}^{-1}$ (figure 3). Based on results from 56 species that covered arctic, boreal, temperate, and tropical biomes, Tjoelker et al (2001) found a negative linear regression between temperature sensitivity of autotrophic respiration and increased growth temperature, with a slope of $-0.046 \text{ }^\circ\text{C}^{-1}$ and an intercept of 3.22. Later, another study with 121 species also found a similar relationship with a slope of $-0.043 \text{ }^\circ\text{C}^{-1}$ and an intercept of 3.09 (Atkin and Tjoelker 2003). Our modeling analysis at the ecosystem level from the northern peatland ecosystem is in line with the findings observed in these studies, and also supports the theory that climate alone can be used to predict the optimal reaction rate, irrespective of plant functional types (Smith et al 2019). Physiological acclimation we found in

this study may be associated with acclimation of newly emerged and overwintered leaves, but not mature leaves of shrub species in this ecosystem (Ward *et al* 2019).

4.2. Ecosystem carbon fluxes under long-term warming

Photosynthetic thermal acclimation can strongly affect ecosystem-atmosphere feedbacks in the global C cycle, especially as the climate warms. The incorporation of thermal acclimation of photosynthetic parameters into a canopy flux model can improve modeled GPP when compared with eddy covariance data (Stinziano *et al* 2018). By fusing the observational C fluxes into the TECO_SPRUCE model, we found the physiological thermal acclimation of $V_{cmaxref}$, J_{maxref} , and entropy in photosynthesis, which resulted in the apparent thermal acclimation of GPP (figure 4(a)). In comparison, if physiological thermal acclimation was not considered, the model would simulate a much higher GPP in response to temperature increase with an increased rate of $22.5 \text{ g C m}^{-2} \text{ yr}^{-1} \text{ }^{\circ}\text{C}^{-1}$ (figure 4(a)). In addition to warming, there are a few other covarying factors that might have contributed to the down-regulation of GPP. First, the lower relative humidity in the warmer treatments caused moss desiccation and consequent smaller coverage of moss (Desai 2014, Norby *et al* 2019). Second, nutrient limitation, though not yet reported at this experiment site, might prohibit a positive effect of warming on GPP (Dusenge *et al* 2019). However, such down-regulation of GPP may not be detected in short-term warming experiments. For example, Johnson *et al* (2013) found two years' warming treatment with infrared lamps significantly increased GPP of the drier, hummock plots whereas had no significant effects on GPP of the wetter, lawn plots in a northern Michigan peatland.

Similar to photosynthetic thermal acclimation, apparent autotrophic respiration was significantly lower at higher temperatures due to a reduced Q_{10Ra} . Opposite to GPP, a slight increase in apparent autotrophic respiration rates would be simulated if thermal acclimation of autotrophic respiration was not taken into account (figure 4(c)). The net effect of an unchanged GPP and decreased R_a under warming was a slow increase in NPP, which was lower than that without incorporating physiological thermal acclimation (figure 4(b)). Increased aboveground NPP (ANPP) of shrub and community-level belowground net primary production have been observed along a gradient of increasing warming in a manipulative mesocosm experiment with intact soil monoliths taken from a bog in northern Minnesota (Weltzin *et al* 2000). However, ANPP of graminoid was found to decrease with increasing warming and ANPP of bryophyte was not affected by warming in the same manipulative experiment (Weltzin *et al* 2000, 2001). Moreover, the responses of NPP to warming in this modeling analysis are inconsistent with that estimated with different components of NPP measured at the same experiment and in the same time period (i.e. 2016–2018), in which warming-induced decreases in aboveground production by trees and the Sphagnum moss community were offset by warming-induced increases in aboveground production by the shrubs and in the belowground production of fine roots of the woody vascular species (Norby *et al* 2019, Hanson *et al* 2020, Malhotra *et al* 2020, McPartland *et al* 2020). Moreover, the increase of NPP under warming simulated in this study is contrasted with a modeling analysis by Jensen *et al* (2019). In their study, by using seasonal, species-specific photosynthesis and respiration parameters measured at this SPRUCE site before the treatments were implemented to parameterize a land surface model, ELM-SPRUCE, ELM-SPRUCE predicted decreased NPP under warming treatments for all four species examined, including two understory shrubs (*R. groenlandicum* and *C. calyculata*) and two overstory trees (*P. mariana* and *L. laricina*). The different responses of NPP to warming among these studies need further investigation, e.g. different measurement methods and/or model intercomparisons.

In contrast to the down-regulation of plant physiological processes, ER, ER, was much higher after adjusting parameters with observational data than that without adjustments of parameters (figure 4(d)). The relative importance of GPP and ER in determining NEE varied. For example, a meta-analysis found that GPP had a greater contribution to NEE than ER under warming (Niu *et al* 2012). In another study, Valentine *et al* (2000) reported that ER dominated the variability in the annual C balance of 15 European forests. In this study in a peatland ecosystem, as a result of the combination of physiological down-regulation under warming and altered parameters for ER by warming, the TECO_SPRUCE model projected a C source of this peatland ecosystem in response to warming at a rate of $28.3 \text{ g C m}^{-2} \text{ yr}^{-1} \text{ }^{\circ}\text{C}^{-1}$, in comparison to a C sink at a rate of $3.5 \text{ g C m}^{-2} \text{ yr}^{-1} \text{ }^{\circ}\text{C}^{-1}$ if the model parameters modified by warming treatments were not incorporated. Estimated ecosystem net C exchange with measured components of net C exchange at the same experiment during the same time period also showed a rapid net carbon loss by $31.3 \text{ g C m}^{-2} \text{ yr}^{-1} \text{ }^{\circ}\text{C}^{-1}$ (Hanson *et al* 2020) and the carbon loss rate has been found to increase to $34\text{--}35 \text{ g C m}^{-2} \text{ yr}^{-1} \text{ }^{\circ}\text{C}^{-1}$ after the measurements in 2019–2021 are incorporated (personal communications with Dr Paul Hanson). However, the carbon loss in the measured net C exchange was dominated by warming-enhanced decomposition losses of CO_2 and enhanced net CH_4 production under warming treatments because NPP did not change under warming (Hanson *et al* 2020), which is consistent with the findings by Johnson *et al* (2013) that the insignificant warming effects on NEE was primarily dominated by the warming effect on ER rather than GPP

in the hummock plots in a northern Michigan peatland. Further studies are needed to explore the slightly different mechanisms for the rapid carbon loss between the simulated and the estimated net C exchange with measurements of its components, i.e. the difference in the contribution of NPP to net C exchange. It should be noted that the initial acceleration in CO₂-C losses via ER in drying and warming in continental bogs may be replaced by the peatland's original CO₂-C sink function because the persistent drought and warming can shift vegetation composition, resulting in increased NPP over time as revealed by Munir *et al* (2015) who compared C fluxes among three sites with contrasting water table levels in a dry continental treed bog.

4.3. Implications for incorporating thermal acclimation into ESMs

It has been well acknowledged that model parameters need to be calibrated with changing temperatures to represent biological thermal acclimation (e.g. Kumarathunge *et al* 2019, Lawrence *et al* 2019, Luo and Schuur 2020). An increasing number of models have begun to incorporate algorithms with dynamic responsive variables that allow models to simulate thermal acclimation of photosynthesis and autotrophic respiration. It is still challenging to parametrize models because of the lack of empirical data available for parameter optimization to implement thermal acclimation of plant photosynthesis and autotrophic respiration. Our study demonstrated an alternative approach to incorporate physiological thermal acclimation by using a process-based ecosystem C cycle model and *in situ* data. This novel method facilitates explorations of how ecosystem fluxes respond to long-term warming. Using warming-induced parameter adjustments had a significant effect on simulated ecosystem fluxes, shifting the peatland ecosystem from C sink to C source. As such, ESMs may overestimate C uptake under global warming if thermal acclimation is not implemented in the models (Liang *et al* 2018). The linear responses of model parameters to changes in temperature in this study are comparable with previous studies and can be implemented into ESMs. Certainly, more ecosystem types need to be investigated in the future to test these algorithms and to collect data needed to better simulate how the global C cycle responds to climate warming and its feedback to climate.

5. Conclusions

In this study, by assimilating observational data from an existing experiment at SPRUCE site involving a gradient of warming treatments into a process-oriented TECO_SPRUCE model, we examined how ecosystem fluxes in the peatland responded to long-term warming. We found thermal acclimation of photosynthesis and autotrophic respiration of plants at the ecosystem level, demonstrated by a linear decrease in temperature sensitivities with warming. The down-regulation of photosynthesis, in combination with increased ER under warming, led to a shift from a C sink to a C source in this peatland ecosystem. Our results at the ecosystem level were consistent with the findings previously observed at the species level and supported the theory that climate alone is a good predictor of the optimal rate of photosynthesis and autotrophic respiration of plants. Without incorporating the thermal acclimation of photosynthesis and autotrophic respiration of plants, ESMs may overestimate the C sequestration capacity of peatlands under warming. Thus, it is critical to incorporate the long-term thermal acclimation of plant physiological processes into ESMs to better predict global C dynamics under future climate and their feedbacks to climate change.

Data availability statement


The data that support the findings of this study are openly available at the following URL/DOI: <http://mnspruce.ornl.gov/>.

Acknowledgments

Part of this research was carried out at the Jet Propulsion Laboratory, California Institute of Technology, under a contract with the National Aeronautics and Space Administration. This work was primarily funded by subcontract CW39470 from Oak Ridge National Laboratory to Cornell University. Oak Ridge National Laboratory is managed by UT-Battelle, LLC, for the U.S. Department of Energy under contract DE-AC05-00OR22725. The SPRUCE (Spruce and Peatland Responses Under Changing Environments) project is supported by the Biological and Environmental Research program in the U.S. Department of Energy's Office of Science.

ORCID iDs

Shuang Ma  <https://orcid.org/0000-0002-6494-724X>
Lifen Jiang  <https://orcid.org/0000-0002-1546-8189>

Rachel M Wilson  <https://orcid.org/0000-0002-5770-9614>
Avni Malhotra  <https://orcid.org/0000-0002-7850-6402>
Yuanyuan Huang  <https://orcid.org/0000-0003-4202-8071>
Feng Tao  <https://orcid.org/0000-0001-6105-860X>
Junyi Liang  <https://orcid.org/0000-0001-8252-5502>
Paul J Hanson  <https://orcid.org/0000-0001-7293-3561>
Yiqi Luo  <https://orcid.org/0000-0002-4556-0218>

References

- Abdalla M, Hastings A, Truu J, Espenberg M, Mander Ü and Smith P 2016 Emissions of methane from northern peatlands: a review of management impacts and implications for future management options *Ecol. Evol.* **6** 7080–102
- Arneeth A, Mercado L, Kattge J and Booth B 2012 Future challenges of representing land-processes in studies on land-atmosphere interactions *Biogeosciences* **9** 3587–99
- Atkin O K, Atkinson L J, Fisher R A, Campbell C D, Zaragoza-Castells J, Pitchford J W, Woodward F I and Hurry V 2008 Using temperature-dependent changes in leaf scaling relationships to quantitatively account for thermal acclimation of respiration in a coupled global climate–vegetation model *Glob. Change Biol.* **14** 2709–26
- Atkin O K, Scheurwater I and Pons T L 2006 High thermal acclimation potential of both photosynthesis and respiration in two lowland *Plantago* species in contrast to an alpine congeneric *Glob. Change Biol.* **12** 500–15
- Atkin O K and Tjoelker M G 2003 Thermal acclimation and the dynamic response of plant respiration to temperature *Trends Plant Sci.* **8** 343–51
- Atkin O, Meir P and Turnbull M 2014 Improving representation of leaf respiration in large-scale predictive climate–vegetation models *New Phytol.* **202** 743–8
- Ball J T, Woodrow I E and Berry J A 1987 A model predicting stomatal conductance and its contribution to the control of photosynthesis under different environmental conditions *Progress in Photosynthesis Research: Volume 4 Proc. 8th Int. Congress on Photosynthesis Providence (Rhode Island, USA, 10–15 August 1986)* ed J Biggins (Dordrecht: Springer) pp 221–4
- Bradford M A, Davies C A, Frey S D, Maddox T R, Melillo J M, Mohan J E, Reynolds J F, Treseder K K and Wallenstein M D 2008 Thermal adaptation of soil microbial respiration to elevated temperature *Ecol. Lett.* **11** 1316–27
- Bridgham S D, Meentemeyer J P, Keller J K, Bliss N B and Trettin C 2006 The carbon balance of North American wetlands *Wetlands* **26** 889–916
- Campbell C, Atkinson L, Zaragoza-Castells J, Lundmark M, Atkin O and Hurry V 2007 Acclimation of photosynthesis and respiration is asynchronous in response to changes in temperature regardless of plant functional group *New Phytol.* **176** 375–89
- Davidson E A and Janssens I A 2006 Temperature sensitivity of soil carbon decomposition and feedbacks to climate change *Nature* **440** 165
- Desai A R 2014 Influence and predictive capacity of climate anomalies on daily to decadal extremes in canopy photosynthesis *Photosynth. Res.* **119** 31–47
- Dusenge M E, Duarte A G and Way D A 2019 Plant carbon metabolism and climate change: elevated CO₂ and temperature impacts on photosynthesis, photorespiration and respiration *New Phytol.* **221** 32–49
- Eliasson P E, McMurtrie R E, Pepper D A, Strömgren M, Linder S and Ågren G I 2005 The response of heterotrophic CO₂ flux to soil warming *Glob. Change Biol.* **11** 167–81
- Farquhar G D, von Caemmerer S and Berry J A 1980 A biochemical model of photosynthetic CO₂ assimilation in leaves of C₃ species *Planta* **149** 78–90
- Friend A D 2010 Terrestrial plant production and climate change *J. Exp. Bot.* **61** 1293–309
- Gelman A and Rubin D B 1992 Inference from iterative simulation using multiple sequences *Stat. Sci.* **7** 457–72
- Granberg G, Grip H, Löfvenius M O, Sundh I, Svensson B H and Nilsson M 1999 A simple model for simulation of water content, soil frost, and soil temperatures in boreal mixed mires *Water Resour. Res.* **35** 3771–82
- Griffiths N A et al 2017 Temporal and spatial variation in peatland carbon cycling and implications for interpreting responses of an ecosystem-scale warming experiment *Soil Sci. Soc. Am. J.* **81** 1668–88
- Hanson P J et al 2017 Attaining whole-ecosystem warming using air and deep-soil heating methods with an elevated CO₂ atmosphere *Biogeosciences* **14** 861–83
- Hanson P J et al 2020 Rapid net carbon loss from a whole-ecosystem warmed peatland *AGU Adv.* **1** e2020AV000163
- Hanson P J, Gill A L, Xu X, Phillips J R, Weston D J, Kolka R K, Riggs J S and Hook L A 2016a Intermediate-scale community-level flux of CO₂ and CH₄ in a Minnesota peatland: putting the SPRUCE project in a global context *Biogeochemistry* **129** 255–72
- Hanson P J, Phillips J R, Brice D J and Hook L A 2018b SPRUCE shrub-layer growth assessments in S1-Bog plots and SPRUCE experimental plots beginning in 2010 (Oak Ridge, TN: Oak Ridge National Laboratory, TES SFA, U.S. Department of Energy) (<https://doi.org/10.25581/spruce.052/1433837>)
- Hanson P J, Phillips J R, Riggs J S, Nettles W R and Todd D E 2014 SPRUCE large-collar *in situ* CO₂ and CH₄ flux data for the SPRUCE experimental plots, carbon dioxide information analysis center (Oak Ridge: Oak Ridge National Laboratory, U.S. Department of Energy) (<https://doi.org/10.3334/CDIAC/spruce.006>)
- Hanson P J, Phillips J R, Wullschelger S D, Nettles W R, Warren J M and Ward E J 2018a SPRUCE tree growth assessments of *Picea* and *Larix* in S1-Bog plots and SPRUCE experimental plots beginning in 2011 (Oak Ridge: Oak Ridge National Laboratory, TES SFA, U.S. Department of Energy) (<https://doi.org/10.25581/spruce.051/1433836>)
- Hanson P J, Riggs J S, Dorrance C, Nettles W R and Hook L A 2015a SPRUCE environmental monitoring data: 2010–2016, carbon dioxide information analysis center (Oak Ridge: Oak Ridge National Laboratory, U.S. Department of Energy) (<https://doi.org/10.3334/CDIAC/spruce.001>)
- Hanson P J, Riggs J S, Nettles W R, Krassovski M B and Hook L A 2015b SPRUCE deep peat heating (DPH) environmental data, February 2014 through July 2105 (Oak Ridge: Oak Ridge National Laboratory, TES SFA, U.S. Department of Energy) (<https://doi.org/10.3334/CDIAC/spruce.013>)
- Hanson P J, Riggs J S, Nettles W R, Krassovski M B and Hook L A 2016b SPRUCE whole ecosystems warming (WEW) environmental data beginning August 2015 (Oak Ridge: Oak Ridge National Laboratory, TES SFA, U.S. Department of Energy) (<https://doi.org/10.3334/CDIAC/spruce.032>)

- Hikosaka K, Ishikawa K, Borjigidai A, Muller O and Onoda Y 2006 Temperature acclimation of photosynthesis: mechanisms involved in the changes in temperature dependence of photosynthetic rate *J. Exp. Bot.* **57** 291–302
- Huang Y, Jiang J, Ma S, Ricciuto D, Hanson P J and Luo Y 2017 Soil thermal dynamics, snow cover, and frozen depth under five temperature treatments in an ombrotrophic bog: constrained forecast with data assimilation *J. Geophys. Res. Biogeosci.* **122** 2046–63
- Huntingford C et al 2017 Implications of improved representations of plant respiration in a changing climate *Nat. Commun.* **8** 1602
- IPCC 2021 *Climate Change 2021: The Physical Science Basis. Contribution of Working Group I to the Sixth Assessment Report of the Intergovernmental Panel on Climate Change* (Cambridge: Cambridge University Press)
- Iversen C M et al 2022 Whole-ecosystem warming increases plant-available nitrogen and phosphorus in an ombrotrophic bog *Ecosystems* **26**
- Iversen C M, Hanson P J, Brice D J, Phillips J R, Mcfarlane K J, Hobbie E A and Kolka R K 2014 SPRUCE peat physical and chemical characteristics from experimental plot cores, 2012 (Oak Ridge, TN: Carbon Dioxide Information Analysis Center, Oak Ridge National Laboratory, U.S. Department of Energy) (<https://doi.org/10.3334/CDIAC/spruce.005>)
- Jensen A M, Warren J M, King A W, Ricciuto D M, Hanson P J, Wulschleger S D and Mäkelä A 2019 Simulated projections of boreal forest peatland ecosystem productivity are sensitive to observed seasonality in leaf physiology *Tree Physiol.* **39** 556–72
- Jiang J, Huang Y, Ma S, Stacy M, Shi Z, Ricciuto D M, Hanson P J and Luo Y 2018 Forecasting responses of a northern peatland carbon cycle to elevated CO₂ and a gradient of experimental warming *J. Geophys. Res. Biogeosci.* **123** 1057–71
- Johnson C P, Pypker T G, Hribljan J A and Chimner R A 2013 Open top chambers and infrared lamps: a comparison of heating efficacy and CO₂/CH₄ dynamics in a northern Michigan peatland *Ecosystems* **16** 736–748
- Johnson F, Eyring H and Williams R 1942 The nature of enzyme inhibitions in bacterial luminescence: sulphanilamide, urethane, temperature, pressure *J. Cell Comp. Physiol.* **20** 247–8
- Kattge J and Knorr W 2007 Temperature acclimation in a biochemical model of photosynthesis: a reanalysis of data from 36 species *Plant Cell Environ.* **30** 1176–90
- King A W, Gunderson C A, Post W M, Weston D J and Wulschleger S D 2006 Plant respiration in a warmer world *Science* **312** 536–7
- Kumarathunge D P et al 2019 Acclimation and adaptation components of the temperature dependence of plant photosynthesis at the global scale *New Phytol.* **222** 768–84
- Larcher W 1980 *Physiological Plant Ecology* (New York: Springer)
- Larigauderie A and Körner C 1995 Acclimation of leaf dark respiration to temperature in alpine and lowland plant species *Ann. Bot.* **76** 245–52
- Lawrence D M et al 2019 The Community Land Model version 5: description of new features, benchmarking, and impact of forcing uncertainty *J. Adv. Model. Earth Syst.* **11** 4245–87
- Liang J et al 2018 Biotic responses buffer warming-induced soil organic carbon loss in Arctic tundra *Glob. Change Biol.* **24** 4946–59
- Lin Y S, Medlyn B E and Ellsworth D S 2012 Temperature responses of leaf net photosynthesis: the role of component processes *Tree Physiol.* **32** 219–31
- Lin Y-S, Medlyn B E, De Kauwe M G and Ellsworth D S 2013 Biochemical photosynthetic responses to temperature: how do interspecific differences compare with seasonal shifts? *Tree Physiol.* **33** 793–806
- Lombardozzi D L, Bonan G B, Smith N G, Dukes J S and Fisher R A 2015 Temperature acclimation of photosynthesis and respiration: a key uncertainty in the carbon cycle-climate feedback *Geophys. Res. Lett.* **42** 8624–31
- Luo Y and Schuur E A G 2020 Model parameterization to represent processes at unresolved scales and changing properties of evolving systems *Glob. Change Biol.* **26** 1109–17
- Luo Y, Wan S, Hui D and Wallace L L 2001 Acclimatization of soil respiration to warming in a tall grass prairie *Nature* **413** 622
- Ma S et al 2021 Satellite constraints on the latitudinal distribution and temperature sensitivity of wetland methane emissions *AGU Adv.* **2** e2021AV000408
- Ma S et al 2022 Evaluating alternative ebullition models for predicting peatland methane emission and its pathways via data-model fusion *Biogeosciences* **19** 2245–62
- Ma S, Jiang J, Huang Y, Shi Z, Wilson R M, Ricciuto D, Sebestyen S D, Hanson P J and Luo Y 2017 Data-constrained projections of methane fluxes in a northern Minnesota peatland in response to elevated CO₂ and warming *J. Geophys. Res. Biogeosci.* **122** 2841–61
- Malhotra A, Brice D, Childs J, Graham J D, Hobbie E A, Vander Stel H, Feron S C, Hanson P J and Iversen C M 2020 Peatland warming strongly increases fine-root growth *Proc. Natl Acad. Sci. USA* **117** 17627–1763410
- McPartland M Y, Montgomery R A, Hanson P J, Phillips J R, Kolka R and Palik B 2020 Vascular plant species response to warming and elevated carbon dioxide in a boreal peatland *Environ. Res. Lett.* **15** 124066
- Melillo J M, Steudler P A, Aber J D, Newkirk K, Lux H, Bowles F P, Catricala C, Magill A, Ahrens T and Morrisseau S 2002 Soil warming and carbon-cycle feedbacks to the climate system *Science* **298** 2173–6
- Mercado L M, Medlyn B E, Huntingford C, Oliver R J, Clark D B, Sitch S, Zelazowski P, Kattge J, Harper A B and Cox P M 2018 Large sensitivity in land carbon storage due to geographical and temporal variation in the thermal response of photosynthetic capacity *New Phytol.* **218** 1462–77
- Metropolis N, Rosenbluth A W, Rosenbluth M N, Teller A H and Teller E 1953 Equation of state calculations by fast computing machines *J. Chem. Phys.* **21** 1087
- Munir T M, Perkins M, Kaing E and Strack M 2015 Carbon dioxide flux and net primary production of a boreal treed bog: responses to warming and water-table-lowering simulations of climate change *Biogeosciences* **12** 1091–111
- Niu S et al 2012 Thermal optimality of net ecosystem exchange of carbon dioxide and underlying mechanisms *New Phytol.* **194** 775–83
- Norby R J and Childs J 2018 SPRUCE: Sphagnum Productivity and Community Composition in the SPRUCE Experimental Plots (Oak Ridge, Tennessee: Oak Ridge National Laboratory, TES SFA, U.S. Department of Energy) (<https://doi.org/10.25581/spruce.049/1426474>)
- Norby R J, Childs J, Hanson P J and Warren J M 2019 Rapid loss of an ecosystem engineer: sphagnum decline in an experimentally warmed bog *Ecol. Evol.* **9** 12571–85
- Oechel W C, Vourlitis G L, Hastings S J, Zulueta R C, Hinzman L and Kane D 2000 Acclimation of ecosystem CO₂ exchange in the Alaskan Arctic in response to decadal climate warming *Nature* **406** 978
- Ofiti N O E, Solly E F, Hanson P J, Malhotra A, Wiesenberg G L B and Schmidt M W I 2022 Warming and elevated CO₂ promote rapid incorporation and degradation of plant-derived organic matter in an ombrotrophic peatland *Glob. Change Biol.* **28** 883–98
- Parsekian A D, Slater L, Ntarlagiannis D, Nolan J, Sebestyen S D, Kolka R K and Hanson P J 2012 Uncertainty in peat volume and soil carbon estimated using ground-penetrating radar and probing *Soil Sci. Soc. Am. J.* **76** 1911–8
- R Core Team 2017 R: a language and environment for statistical computing (available at: www.R-project.org/)

- Ricciuto D M *et al* 2021 An integrative model for soil biogeochemistry and methane processes: i. Model structure and sensitivity analysis *J. Geophys. Res. Biogeosci.* **126** e2019JG005468
- Scafaro A P, Xiang S, Long B M, Bahar N H A, Weerasinghe L K, Creek D, Evans J R, Reich P B and Atkin O K 2017 Strong thermal acclimation of photosynthesis in tropical and temperate wet-forest tree species: the importance of altered Rubisco content *Glob. Change Biol.* **23** 2783–800
- Sebestyen S D, Dorrance C, Olson D M, Verry E S, Kolka R K, Elling A E and Kyllander R 2011 *Long-term Monitoring Sites and Trends at the Marcell Experimental Forest* (New York: CRC Press)
- Shi Z, Yang Y, Zhou X, Weng E, Finzi A C and Luo Y 2015 Inverse analysis of coupled carbon-nitrogen cycles against multiple datasets at ambient and elevated CO₂ *J. Plant Ecol.* **9** 285–95
- Smith N G *et al* 2019 Global photosynthetic capacity is optimized to the environment *Ecol. Lett.* **22** 506–17
- Smith N G and Dukes J S 2013 Plant respiration and photosynthesis in global-scale models: incorporating acclimation to temperature and CO₂ *Glob. Change Biol.* **19** 45–63
- Smith N G, Malyshev S L, Shevliakova E, Kattge J and Dukes J S 2015 Foliar temperature acclimation reduces simulated carbon sensitivity to climate *Nat. Clim. Change* **6** 407
- Stinziano J R, Way D A and Bauerle W L 2018 Improving models of photosynthetic thermal acclimation: which parameters are most important and how many should be modified? *Glob. Change Biol.* **24** 1580–98
- Tjoelker M G, Oleksyn J and Reich P B 1999 Acclimation of respiration to temperature and CO₂ in seedlings of boreal tree species in relation to plant size and relative growth rate *Glob. Change Biol.* **5** 679–91
- Tjoelker M G, Oleksyn J and Reich P B 2001 Modelling respiration of vegetation: evidence for a general temperature-dependent Q₁₀ *Glob. Change Biol.* **7** 223–30
- Valentini R *et al* 2000 Respiration as the main determinant of carbon balance in European forests *Nature* **404** 861–5
- Wang Y P and Leuning R 1998 A two-leaf model for canopy conductance, photosynthesis and partitioning of available energy I: model description and comparison with a multi-layered model *Agric. For. Meteorol.* **91** 89–111
- Ward E J, Warren J M, McLennan D A, Dusenke M E, Way D A, Wullschlegel S D and Hanson P J 2019 Photosynthetic and respiratory responses of two bog shrub species to whole ecosystem warming and elevated CO₂ at the boreal-temperate ecotone *Front. For. Glob. Change* **2** 54
- Weltzin J F, Harth C, Bridgham S D, Pastor J and Vonderharr M 2001 Production and microtopography of bog bryophytes: response to warming and water-table manipulations *Oecologia* **128** 557–65
- Weltzin J F, Pastor J, Harth C, Bridgham S D, Updegraff K and Chapin C T 2000 Response of bog and fen plant communities to warming and water-table manipulations *Ecology* **81** 3464–78
- Weng E and Luo Y 2008 Soil hydrological properties regulate grassland ecosystem responses to multifactor global change: a modeling analysis *J. Geophys. Res. Biogeosci.* **113** G03003
- Xu T, White L, Hui D and Luo Y 2006 Probabilistic inversion of a terrestrial ecosystem model: analysis of uncertainty in parameter estimation and model prediction *Glob. Biogeochem. Cycles* **20** GB2007
- Yuan F H, Wang Y H, Ricciuto D M, Shi X Y, Yuan F M, Hanson P J, Bridgham S, Keller J, Thornton P E and Xu X F 2021 An integrative model for soil biogeochemistry and methane processes. II: warming and elevated CO₂ effects on peatland CH₄ emissions *J. Geophys. Res. Biogeosci.* **126** e2020JG005963
- Ziehn T, Kattge J, Knorr W and Scholze M 2011 Improving the predictability of global CO₂ assimilation rates under climate change *Geophys. Res. Lett.* **38** L10404